

System design of a mission to detect Earth-sized planets in the inner orbits of solar-like stars

David Koch, et al

Note added by author: Since this paper was accepted for publication, a major change was made in the mission design. The spacecraft was lightened by removal of the propulsion stage. The launch vehicle was changed to a Delta-Lite and the orbit changed to a heliocentric orbit, thereby reducing the overall costs.

In addition the threshold was changed (the hardware was not) so that data from 14th magnitude stars will be recorded. This increases the number of stars for which earth-sized transits can be detected from 5000 to 16,000. It was also learned that the number of stars for which 2.2x earth-radii planets or larger could be seen is 34,000. (The increase coming from inclusion of late A and all the F dwarfs.) And finally, by inclusion of M-dwarfs, 12,000 stars can be monitored for Mars size or larger. Thus the total for earth-sized or larger is 28,000 and for 2.2x earth radii the number is 62,000.

Finally, objects such as 51 Peg have now been detected with orbits as close in as 1/20 of an AU. Orbits this close in have a 10% random chance of being aligned along the line of sight. Thus it is anticipated that 70 inner-orbit major planets as well as 50 outer-orbit major planets will be detected. Radial velocity measurements for the inner and astrometry measurements for the outer can be used to obtain the planet's mass and in combination with the size from photometry, the planet's density can be calculated.

The up-to-date mission description can be found on-line at www.kepler.arc.nasa.gov

System design of a mission to detect Earth-sized planets in the inner orbits of solar-like stars

David Koch, William Borucki, Kent Cullers¹, Edward Dunham², and Larry Webster
Space Science Division, NASA Ames Research Center, Moffett Field, California

Tom Miers and Harold Reitsema
Ball Aerospace, Boulder, Colorado

Abstract. A point design for a mission to detect Earth-sized planets in the inner orbits of solar-like stars is described. The observing technique is based upon continuously and simultaneously monitoring 5000 solar-like stars for brightness changes that would be caused by planets transiting their star. Detection of periodic transits of the same amplitude and duration provides for a robust method of discovery. The instrument would consist of a 1-m Schmidt telescope with an array of charge-coupled devices (CCDs) filling the 12° field of view. The instrument would be placed in a halo orbit about the L2 Lagrange point, where its viewing would not be obscured at any time by the Sun, Earth, or Moon.

Background of the Investigation

Given the NASA Administrator's continuing imperative (initially stated by D. Goldin, invited talk, AGU, May 26, 1994, Baltimore, Md., 1994) to image an Earth-like planet, it appears reasonable that a step in that direction would be to first determine the existence of Earth-like planets prior to embarking on a program to image them. Further, from a scientific standpoint, determination of the properties of the individual planets and of planetary systems as a whole is as important as obtaining an image of a planet. Thus a practical point design for a mission to determine the Frequency of Earth-Sized Inner Planets (FRESIP), especially those in the inner orbits of solar-like stars, has been developed. The point design fits well within the constraint envelope for a NASA Discovery-class mission.

The point design presented herein permits continuous and simultaneous monitoring of 5000 solar-like stars for evidence of brightness changes due to the transits of Earth-sized planets of solar-like stars. When a pair of transits is detected, the prediction and detection of a third and all subsequent transits for that system can be made. This periodic repeatability leads to a high level of confidence of discovery. The probability for detecting transits is quite favorable for planets in inner orbits, that is, from a fraction of an AU to a few AUs, which includes the habitable zone, a region where liquid water is expected to exist on a planet. If other planetary systems are similar to our own, then approximately 1% of those systems will show transits [Borucki and Summers, 1984]. Thus this mission design should be capable of discovering 50 Earth-sized planets in the inner orbits of solar-like stars. A full description of the scientific basis for the mission is elsewhere [Borucki et al, 1996].

Photometric Precision Requirements

The brightness reduction due to a transit is proportional to the ratio of the planet's area to that of the star's. For stars the size of the Sun, the decrease in light amounts to approximately 1% for

giant planets such as Jupiter and Saturn, 0.1% for planets like Uranus and Neptune, and 0.01% for planets like Earth and Venus. The design requirement for a system (detector plus star) is to have a 1-sigma noise level of 1:50,000 so that the change in brightness due to a transit of an Earth-sized body ($L/L=1/12,000$) will result in a 4-sigma detection per 4-hour integration interval for the faintest stars. This level of precision includes all noise factors described below. To obtain the precision required to detect Earth-sized planets, the photometric system must also avoid the scintillation limit incurred by ground-based observations [Young 1974]. Even more limiting for ground-based observations is atmospheric transparency variations due to large air mass changes over the periods relevant to planetary transit detection. The precision for about a 12-hour period is less than one part in 1000 for ground based observations even when extreme measures are taken to minimize photometric drifts [Gilliland et al., 1991]. The day-night cycle and seasonal effects also make it essentially impossible to continuously monitor a single group of stars for the several years needed for reliable planet detection. Thus a space-based mission is needed to achieve the required observations.

System Noise

The major sources of noise that are expected to compete with the transit signal are stellar variability, photon shot noise, detector noise, and pointing equivalent noise. Since they are not correlated, they can be combined in a root sum square (RSS) as given by

$$(\text{Sys Noise})^2 = (\text{Stellar Var})^2 + (\text{Shot Noise})^2 + (\text{Det Noise})^2 + (\text{Pointing Noise})^2. \quad (1)$$

The noise budget for the faintest target star for 4-hour integrations is allocated as

stellar variability = 1 part in 100,000
photon shot noise = 1 part in 71,000
detector noise = 1 part in 150,000
pointing equivalent noise = 1 part in 150,000.

Selection of spectral type and stellar variability.

Solar-like stars, especially the later spectral types, are among the quietest stars known. For a magnitude limited survey, most of the stars in the Galaxy are well behaved main-sequence F-, G- and K-

¹Now at SETI Institute, Mountain View, California

²Now at Lowell Observatory, Flagstaff, Arizona

Copyright 1996 by the American Geophysical Union

Paper number 96JE00468.

0148-0227/96/96JB-00468\$09.00

dwarf stars. If these solar-like stars have a variability similar to that of the Sun, then the intrinsic brightness fluctuations are expected to range from 10^{-3} at the rotational period of the star due to the presence of large sunspot groups to values of less than 10^{-5} with a duration of several hours due to turbulent motions and gravity waves in the stellar atmosphere [Frohlich, 1987]. The durations of planetary transits range from 4 hours for a Mercury grazing transit to 16 hours for a Mars central transit. Thus stellar brightness variations of duration greater than 16 hours will not substantially affect the detectability of transits. Variations less than about 4 hours will be too small to have an effect.

Although effects of star spots will be observed and could show brightness variations larger than those from transits by small planets, their presence would cause difficulty only for stars with short rotation periods. Studies show that rotation periods increase with age [Soderblom *et al.*, 1993] and become quite long for stars later than spectral class F0 [Simon *et al.*, 1985]. Spectral classes F5 through K5 have periods of weeks, similar to that of the Sun, and the presence of spots should not prevent the detection of planetary transits. Many of the stars earlier than F5 have rotation periods shorter than weeks, but these stars generally also have a lower level of activity in the CaII H & K lines. Because this activity can be related to the intensity of spot cycles [Noyes *et al.*, 1984], it is believed that spectral class F dwarfs are likely to be quieter than the Sun, a G2 dwarf star.

The active cavity radiometer for irradiance monitoring (ACRIM I) aboard the Solar Maximum Mission (SMM) satellite was used to measure the total solar flux integrated over all wavelengths [Willson *et al.*, 1981; Willson and Hudson, 1991]. These measurements show the solar variability to be less than one part in 100,000 for periods of 12 hours or less (see Figure 1). No data on any other star equal or better this precision. The minute-by-minute data for the 5-year interval from January 1985 to July 1989 from the ACRIM I radiometer were obtained directly from R. Willson. These data span a time from the minimum of the

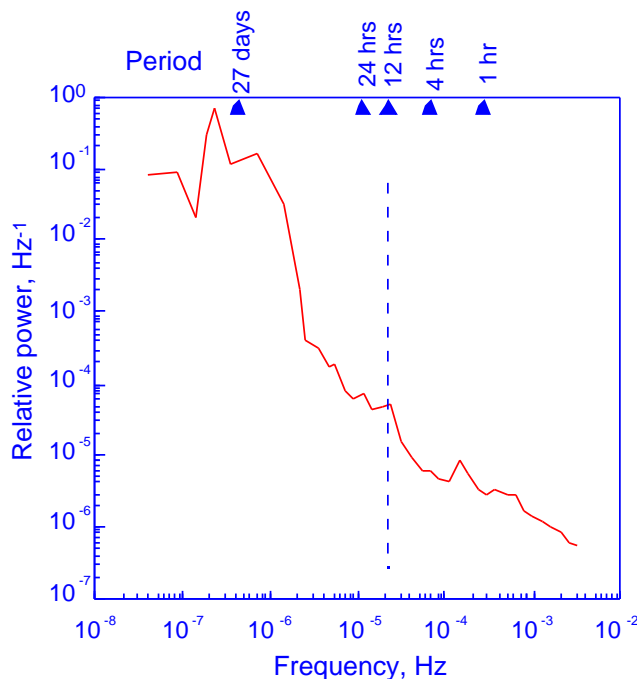


Figure 1. Power spectrum of the Sun from the ACRIM I, SMM data. The intrinsic peak variability of the Sun is of the order of one part in 1000, and the relative intensity (square root of the power) on timescales for a transit (12 hours) is a factor of 100 less; thus the variability is of the order of one part in 100,000 [Reproduced from Woodard *et al.*, 1982; Used with permission from Joint Institute for Laboratory Astrophysics].

solar activity cycle to near maximum. Because the ACRIM I data included the UV portion of the spectrum, these data are expected to be 30% more variable than that expected with the UV excluded.

Since much of the variability in solar-like stars has been found to occur in the UV, such as the CaII H & K lines, the short-wavelength cutoff for the instrument will be at 0.4 microns to reduce the effects of these variations. Thus, for this mission the measurements will be broad-band and white-light to both minimize effects of variability due to lines as well as to collect the maximum number of photons to meet the necessary statistical precision.

Photon shot noise. Statistical noise is determined by the number of photons counted. The desired noise level is achieved by recording enough counts per integration interval for the faintest acceptable star. To achieve 1 part in 10^5 requires recording of 10^{10} counts. The minimum integration time required to obtain these counts is 4 hours, the interval for a grazing transit at 0.3 AU. The telescope 1-m aperture and optical efficiency, and the detector band pass of 0.4 to 1 micron and quantum efficiency determine the sensitivity to be about 12.5 stellar magnitudes. A star field has been selected that contains 5000 solar-like stars brighter than 12.1 magnitudes. A number of alternate fields require the 12.5 magnitude sensitivity.

Detector noise. Laboratory tests of charge-coupled devices (CCDs) were conducted at the flux levels and time durations expected to demonstrate that off-the-shelf CCDs have the photometric precision required. Independent groups working at Ball Aerospace and Lick Observatory performed tests using relative photometry of artificial star fields (taking a ratio of the flux of an individual star to that of all other stars on the CCD). It was found that the dominant error source in the experiments was image motion, such as that caused by flexure of the mechanical system as the cryogenic coolant boiled off. By accurately centroiding star images and fitting a linear function of the relative photometry to the image position, combined with a term which fit an observed nonlinearity in CCD response as a function of brightness, the groups demonstrated that both front- and back-illuminated CCDs can routinely provide near shot-noise limited performance. The residual noise for the 21 smallest stars produced by a mask with 127 holes of various sizes is presented in Figure 2. The figure shows that the required detector noise level of 1:150,000 should be achievable, since a level of 1:100,000 has already been obtained without any attempt to optimize the detector [Robinson *et al.*, 1995].

During the mission, as in the laboratory, relative photometry will be used to eliminate effects of changes in the system gain. The amplitude of each star will be compared to the amplitude of the ensemble of stars (typically, 250 per CCD) within each CCD. Biases in the CCDs will be removed using overclocking and sampling of background areas. Changes in the photometric accuracy on timescales long relative to a day are not important for detection of transits. However, it will be essential to maintain the photometric precision on timescales of hours.

Pointing equivalent noise. Pointing jitter affects the photometric precision in two ways. Target stars are not isolated in space and will have adjacent faint background stars. As the telescope wanders ever so slightly on the sky about its pointing direction, images of the background stars will move both onto and off of the pixels used for each target star. Likewise, some of the light from the target star will move off of the target pixels. An analysis of this effect, which depends on the luminosity function (stellar distribution in the galaxy), CCD characteristics, and telescope design, indicates a 3-sigma pointing stability requirement of 0.3 arc sec. With the stellar image defocused by five pixels, no more than 10% of the potential target stars would be lost owing to a contaminating adjacent star. A second effect depends on the CCD subpixel variations in sensitivity [Jorden *et al.*, 1994] and affects the measured signal as the stellar image

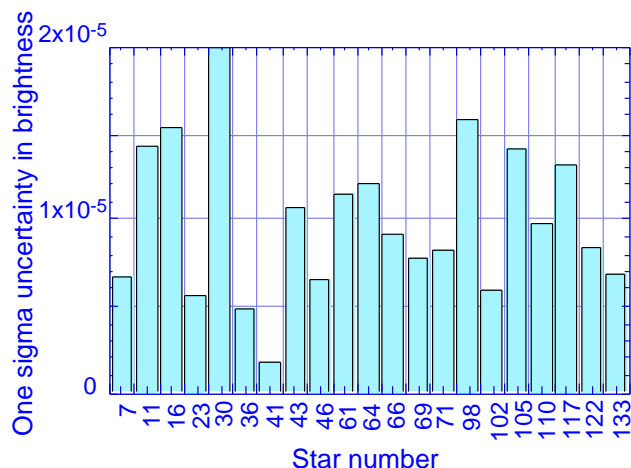


Figure 2. CCD noise measurements. Tests were performed over 10 days to measure the intrinsic noise of off-the-shelf CCDs. A mask with 127 apertures was used to generate simulated stars. The brightnesses for the 21 smallest stars were normalized to all of the stars for each integration (41 min) to remove light source variations. Corrections were applied for image motion and samples combined into 5-hour integrations with quadratic subtraction of shot noise. The average noise was found to be 0.99×10^{-5} [Reproduced from *Robinson, et al.*, 1995. Copyright 1995, Astronomical Society of the Pacific; used with permission.].

moves on the CCD. Defocusing of the image by several pixels reduces this effect as well as increases the allowed integration time between CCD readouts. The selection of a halo orbit about L2 eliminates many of the perturbing torques associated with Earth-orbiting telescopes, such as those due to atmospheric drag, gravity gradients and magnetic moments. This leaves solar radiation pressure the dominant factor, which will cause a very small torque owing to the difference of the geometric center from the center of mass of the spacecraft. Finally, the spacecraft does not have any deployable or articulated components which would also contribute to pointing instability.

Simulated Transit Events

The detectability of single and multiple transit events is illustrated in Figure 3. Plotted in the top section of the figure are four simulated transit events. Each simulation includes the four noise sources expected in the data: pointing noise, CCD noise, photon (shot) noise, and stellar variability. The noises are based on the use of a 4-hour integration time. The simulations are generated by algebraically adding two data sets: CCD laboratory data of artificial stars with an intrinsic CCD fractional error of 1.3×10^{-5} , and solar variability data from SMM with a fractional error of 0.7×10^{-5} . Pointing noise with a fractional error of 1×10^{-5} is added to the CCD data through image motion (0.55 pixels or 0.16 arc sec). Because the SMM data have no appreciable photon noise, a Gaussian distributed random noise is added to simulate the expected photon noise (1.4×10^{-5}). The RSS sum of the errors (see equation (1)), is 2.26×10^{-5} , which is in good agreement with both the budgeted error of 2.0×10^{-5} , and the error measured in the simulations, which had a mean of 2.15×10^{-5} . All quantities are binned into 4-hour intervals and a 12-hour Earth-sized transit of 8.0×10^{-5} was added to the data. Multiple simulations show that, on average, a single transit event of 4 hours is a 3.5-sigma detection for a star at the limiting magnitude of the system. Note that while the data are binned into 4-hour intervals, the time resolution for locating event centers is much better, as the integrated brightness for target stars is taken with 15-min centers.

The bottom plot in Figure 3 shows the result of combining or "folding" four transit data strings together. The result is a 7.5-sigma detection, such that 83% of planetary transits will be detected with four transits for the stars at the limiting magnitude of the system. This simulation utilizes real solar variability and real CCD noise, demonstrating that CCDs can consistently operate at the precision level necessary for the mission and that solar-type stars are sufficiently quiet to allow detection of transits of Earth-sized planets.

Whatever inherent variability is seen in the data, it can be reduced by folding of the data for the range of periods of interest to permit detection of planets at the limiting sensitivity if the stellar noise becomes greater or for detection of planets even smaller than the Earth. For a planet in a Mercury-like orbit and for an 8-year mission there would be 32 transits in the data. Thus a planet 5.6 times smaller in area than the Earth could be detected. That is, a Mars could be detected if it were in a Mercury-like orbit. The sensitivity will be even better for stars that are brighter than those at the limiting magnitude.

Instrument, Spacecraft, and Mission Design

Instrumentation

The instrument will measure the brightnesses of 5000 solar-like stars using a wide field-of-view (FOV) telescope and a CCD photometer. The enabling new technologies that make this mission feasible are high-photometric-precision, large format CCDs and ultralightweight optics. To continuously and simultaneously monitor 5000 target stars and to capture enough photons during the transit period to meet the precision requirement, a 1-m aperture telescope with a 12° FOV is necessary. The optics will consist of a 1-m diameter Schmidt corrector plate, a 1.4-m-diameter primary mirror, and individual field-flattening lenses for each of the 21 CCDs at the focal plane. Only data from the pixels on which the 5000 stars are imaged will be recorded onboard and later telemetered to the ground. Eight bytes of data per star are used for each 15-min integration, yielding 4 megabyte (MB) per day of primary science data for 5000 stars. The estimated mass of the instrument is 300 kg plus 33% margin. A summary of the system is given in Table 1.

Spacecraft Design

The spacecraft design, illustrated in Figure 4, is low-risk and takes full advantage of the most recent technology and off-the-

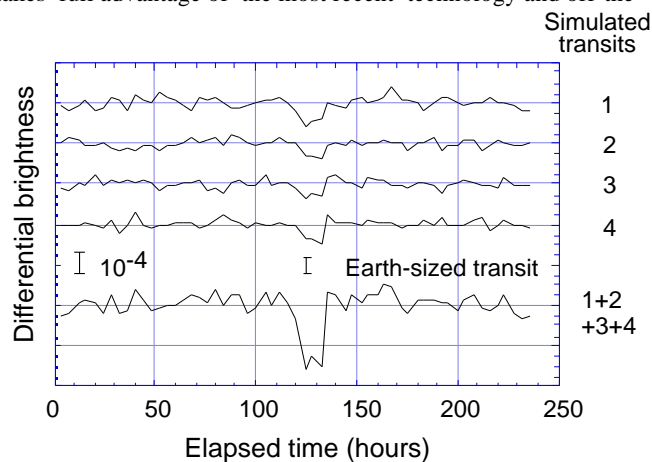


Figure 3. Detectability of transit events. Four independent simulations of an Earth-sized transit are shown. The data contain actual CCD noise and solar variability from SMM data. Gaussian shot noise and pointing equivalent noise are added. The bottom trace is a sum of the four separate data sets.

Table 1. Mission Design Summary

	Component	Specification
Focal plane	Detector	21 - 2048 x 2048 CCDs (24 micron pixels)
	Operating temperature	-40°C
	Read noise	<15 e ⁻ /rms
	Dark current noise	<100 e ⁻ /pixel/s
Telescope	Type	Schmidt
	Primary mirror	1.40 m diameter
	System f/#	1.47
	Focal length	1.4 m
	Active FOV	84 deg ²
Spacecraft	Type	Custom with integrated instrument
	Instrument mass	300 kg plus 33% margin
	Instrument power	250 W continuous
	Fine pointing system	Star tracker CCD on focal plane
	Total data rate	10 MB/d
Mission	Lifetime	Design for 4 years (reliability) Expendables for 8 years
	Observing mode	Single fixed inertial target FOV
	Orbit type	Halo about Sun-Earth L2 Lagrange point
	Launch vehicle	Delta II 7920 with 9.5 ft fairing

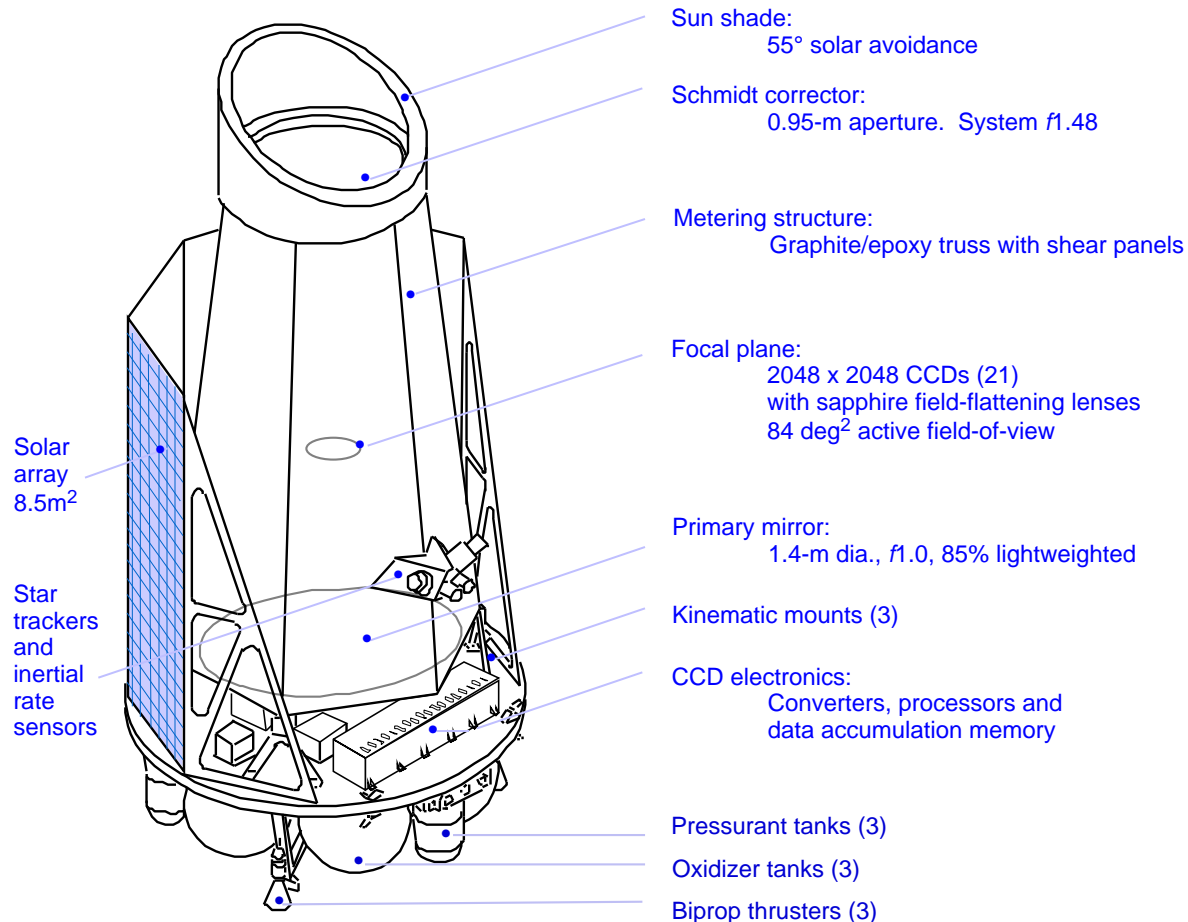
shelf, flight-proven hardware. To reduce operational risk and minimize pointing jitter, there are no articulated or deployable mechanisms on the spacecraft or instrument. The total mass of the instrument and spacecraft is 1455 kg, including 33% margin for the instrument, a propulsion system to transfer the spacecraft

from Earth orbit to an L2 trajectory, and 20% margin for the spacecraft reserves.

To minimize the solar panel size, avoid articulated arrays and keep the arrays illuminated while the telescope is pointed to the inertially fixed position on the sky, the spacecraft will be rotated 90° about the telescope axis (matching the focal plane symmetry) every 3 months. This rotation will provide a nearly constant thermal environment for the instrument and spacecraft. Wrapping the solar array around half of the instrument and keeping the Sun within a single 90° range will add thermal protection and thereby simplify the thermal design. A fixed 35° sunshade will prevent any sunlight from entering the telescope optics or solar-radiation heating of the Schmidt corrector.

Power usage will be nearly constant, and the solar arrays will be constantly illuminated. The 8.5 m² of solar array provides 33% reserves at end-of-life. Since the instrument stares at a single field in the sky, there is no need to slew or retarget the instrument. Therefore small ultralow noise reaction wheels can be used. Every 3 months a 90° roll is required to compensate for solar motion due to orbital motion, and about twice per year, attitude control system support is required for halo orbit maintenance. The data compression resulting from onboard data extraction for only those pixels of interest results in a total of only 4 MB of primary science data per day. These data will be transmitted with a medium-gain, nonarticulated antenna.

Three levels of propulsion are required: injection toward the halo orbit from Earth orbit, transfer trajectory trim and halo orbit station keeping; and reaction wheel desaturation. The first will be accomplished with a bipropellant system; the second with hydrazine and the third using cold gas. Half of the total spacecraft mass is accounted for by the propulsion stage.

**Figure 4.** Isometric drawing of the spacecraft and telescope.

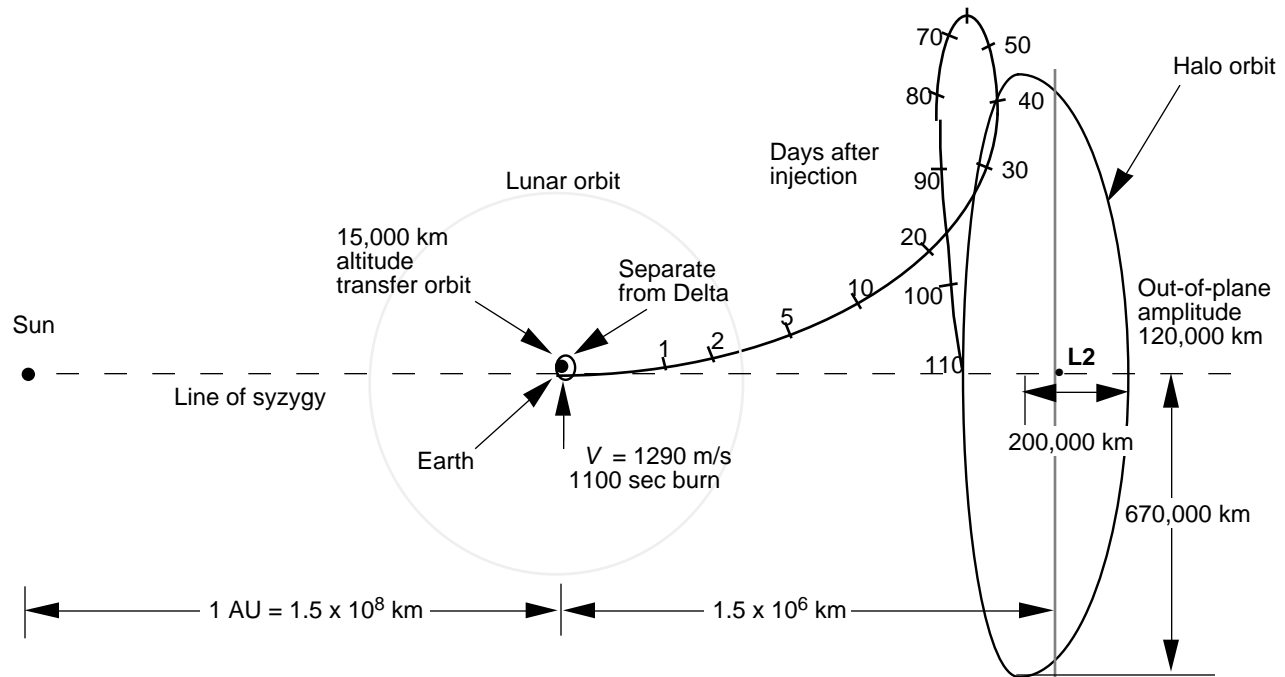


Figure 5. Geometry and time line for an L2 halo orbit. The L2 Lagrange point is on the Sun-Earth line of syzygy at about 0.01 AU (1.5×10^6 km) from the Earth. A halo orbit about this point is three dimensional, with coupled two-dimensional periodic motion in the ecliptic plane and independent periodic motion out of the ecliptic, thus describing a three-dimensional Lissajous figure. The amplitudes can be chosen such that the frequencies become equal and with appropriate phasing, the spacecraft will appear to be orbiting about the line of syzygy. The minimum in-plane amplitude must be of the order of 670,000 km, about 24° from the line of syzygy. The halo orbital period of 180 days is somewhat less than half the Earth's orbital period. Injection into a large-amplitude halo orbit requires a $V \sim 50$ m/s, far less than that needed for placement at L2 (~ 300 m/s). Orbital maintenance requires a $V \sim 10$ m/s/yr. Locations along the trajectory from Earth orbit are indicated in days.

Mission Operations Design

The continuous viewing needed for a high detection efficiency for planetary transits requires that the field-of-view (FOV) be out of the ecliptic plane so as not to be blocked periodically by the Sun or the Moon. A star field near the galactic plane that meets these viewing constraints and has a sufficiently high star density has been selected. A halo orbit about the Sun-Earth L2 Lagrange point (see Figure 5) provides the optimum approach to meeting the combined Sun-Earth-Moon avoidance criteria within the Delta launch vehicle capability and avoids the high radiation dosage associated with an Earth orbit. The halo orbit has substantial heritage, based on the ISEE 3 (later ICE) and Wind missions and the planned use for the Solar and Heliospheric Observatory (SOHO) and Advanced Composition Explorer (ACE) missions [Farquhar and Dunham, 1990]. Telemetry and navigation for the mission will be via the Deep Space Network (DSN).

The flight system will be launched on a Delta II two-stage launch vehicle into a highly elliptical Earth orbit. Once separated from the Delta II, the spacecraft will use its own bipropellant system to leave Earth orbit. The transfer to the halo orbit about the L2 Lagrange point will require 110 days. Spacecraft check out will occur shortly after leaving Earth orbit, and first light and calibration of the focal plane will begin by day 14. Science operations to detect Earth-sized transits will then commence. Mission operations will be conducted from NASA Ames Research Center.

Conclusion

Detection of Earth-sized planets in inner orbits of solar-like stars by observing planetary transits is both a very practical and a robust method for discovering of extrasolar planetary systems.

With progress both in the understanding of solar variability, indicating that similar variations in solar-like stars should not mask Earth-sized transits, and progress in laboratory measurements of the precision achievable with large-format CCDs, a practical space-based photometry mission for transit detection with a precision of one part in 50,000 is feasible. The concept presented is not only practical but fits well within the envelope of a NASA Discovery-class mission. Results from such a mission should discover approximately 50 Earth-sized planets and provide the impetus and justification for a more ambitious mission to image Earth-sized planets. If, on the other hand, no Earth-sized planets are detected, then the null result would have equally profound implications.

References

- Borucki, W. J., and A. L. Summers, The photometric method of detecting other planetary systems, *Icarus*, 58, 121, 1984.
- Borucki, W. J., K. Cullers, E. W. Dunham, D. G. Koch, W. D. Cochran, A. Granados, and J. A. Rose, FRESIP: A mission to determine the character and frequency of extrasolar planets around solar-like stars, *Space Sci Rev*, in press, 1996.
- Farquhar, R. W., and D. Dunham, Use of libration-point orbits for space observations, in *Observatories in Earth Orbit and Beyond*, IAU Colloq. 123, edited by Y. Kondo, p. 391, Int. Astron. Union, Paris, 1990.
- Frohlich, C., Variability of the solar "constant" on timescales of minutes to years, *J. Geophys. Res.*, 92, 796, 1987.
- Gilliland, R. L., T. M. Brown, D. K. Duncan, N. B. Suntzeff, G. W. Lockwood, D. T. Thompson, R. E. Schild, W. A. Jeffrey, and B. Penprase, Time-resolved CCD photometry of an ensemble of stars in the open cluster M67, *Astron. J.* 101, 541, 1991.
- Jorden, P. R. J., Deltorn, and A. P. Oates, The non-uniformity of CCDs

- and the effects of spatial undersampling, *Instrum. Astron.* VIII, SPIE, Proc. Int. Soc. Opt. Eng., 2198, 1994.
- Noyes, R. W., L. W. Hartmann, S. L. Baliunas, D. K. Duncan, and A. N. Vaughn, Rotation, convection, and magnetic activity in lower main-sequence stars, *Astrophys. J.*, 279, 763, 1984.
- Robinson, L. B., M. Z. Wei, W. J. Borucki, E. W. Dunham, C. H. Ford, and A. F. Granados, Test of CCD precision limits for differential photometry, *P Astron. Soc. Pac.*, 107, 1094, 1995.
- Simon, T., G. Herbig, and A. M. Boesgaard, The evolution of chromospheric activity and the spin-down of solar-type stars, *Astrophys. J.*, 293, 551, 1985.
- Soderblom, D. R., J. R. Stauffer, K. B. MacGregor, and B. F. Jones, The evolution of angular momentum among zero-age main-sequence solar-type stars, *Astrophys. J.*, 409, 624, 1993.
- Willson R. C. and H. S. Hudson, The sun's luminosity over a complete solar cycle, *Nature*, 351, 42, 1991.
- Willson, R. C., S. Gulkis, M. Janssen, H. S. Hudson, and G. A. Chapman, Observations of solar irradiance variability, *Science*, 211, 700, 1981.
- Woodard, M., H. S. Hudson, and R. Willson, Variability of solar total irradiance, in *Proc. Conf. on Pulsating Stars and Cataclysmic Variables*, edited by J. P. Cox and C. J. Hansen, p. 152, Joint Inst. for Lab. Astrophys., Boulder, Colo., 1982.
- Young, A. T., Other components in photometric systems, in *Methods of Experimental Physics*, vol. 12A, edited by N. Carlton, p. 95, Academic, San Diego, Calif., 1974.
- W. Borucki, D. Koch, and L. Webster, NASA Ames Research Center, MS 245-6, Moffett Field, CA 94035 (e-mail: koch@chandon.arc.nasa.gov)
- K. Cullers, SETI Institute, 2035 Landings Drive, Mountain View, CA. 94043
- E. Dunham, Lowell Observatory, 1400 W. Mars Hill Rd., Flagstaff, AZ 86001.
- Tom Miers and Harold Reitsema, Ball Aerospace, P. O. Box 1062, Boulder, CO 80306

(Received August 2, 1995; revised February 5, 1996;
accepted February 6, 1996.)